Computational Investigation of Ethylene Insertion into the Metal−Methyl Bond of First-Row Transition Metal(III) Species

Vidar R. Jensen* and Walter Thiel

Max-Planck-Institut für Kohlenforschung, Kaiser-Wilhelm-Platz 1, D-45470 Mülheim an der Ruhr, Germany

Received June 15, 2001

Ethylene coordination and insertion into the transition metal−methyl bond have been investigated using nonlocal density functional theory (DFT) for the lowest spin states of $[(\eta^1,\eta^5\text{-}H_2NC_2H_4C_5H_4)M(III)Me]^+$ (M = Sc−Co) compounds. Benchmark tests at the CASPT2 level confirm that a DFT approach with correction of spin contamination adequately describes the potential surfaces for this reaction as well as the separation of the various spin states. The calculations demonstrate the importance of having a single low-lying unoccupied frontier orbital available for bond formation in the π complex and the transition state (TS) region. A reactant complex with nine occupied valence orbitals around the metal, present for example in the high-spin d^4 configuration, is not expected to act as an efficient olefin polymerization catalyst. An empty orbital can, however, be created by spin pairing, which then allows the formation of a π complex with a covalent metal−ethylene bond. This bond must be broken during insertion, and as a result, high barriers for the low-spin complexes are to be expected. The calculations are consistent with observations for existing M(III)-based olefin polymerization catalysts. Highly active catalysts are predicted for Sc and also for V and Co, whereas Mn(III) complexes are not expected to show significant activity.

1. Introduction

As we approach the 50th anniversary of the discovery of transition metal-catalyzed olefin polymerization, new examples are being reported at an ever increasing rate. The search has been driven mainly by the desire to control the structure and properties of the resulting polymer rather than to increase the activity of the catalyst. Since no single catalytic system can generate the whole spectrum of different polymers, the main aim has been to develop catalysts involving new metals and ligands, and as a result, a whole range of catalysts is now available for tailor-making polyolefins.[1]

To analyze differences and trends among the new catalysts, they need to be classified. One possible criterion is the formal oxidation state of the metal. This is attractive from a theoretical point of view since for a single oxidation state, it is possible to systematically study both the electronic and steric effects of different ligands as well as the electronic effects resulting from the use of different metals with a varying number of d electrons. The latter strategy is used in the current contribution.

Historically, the oxidation state IV has received most attention: the first-generation Ziegler catalysts, $TiCl_4/AlR_3$,[2] fall into this category, as do the ubiquitous group IV metallocene-based catalysts.[3] However, the catalysts used in the technically important shell higher olefin process (SHOP) for the oligomerization of ethylene are based on Ni(II),[4] and the recent development of the highly active cationic, bidentate α-diimine catalysts of nickel and palladium as well as the tridentate analogues of iron and cobalt[5] has further emphasized the importance of the oxidation state II. Reports on catalysts based on the oxidation state III have been scarce in comparison, and only recently have highly active, homogeneous, well-defined M(III)-based catalysts for the polymerization[6−9] and oligomerization[10,11] of ethylene been developed. These catalysts contain 6+2-electron donor-substituted cyclopentadienyl (Cp) ligands, with chromium[7−10] or titanium[6] as the metal. Using a ligand design found in the successful Cr(III) and Ti(III) catalysts, the main goal of the current contribution is to identify other first-row transition metals having oxida-

(1) Britovsek, G. J. P.; Gibson, V. C.; Wass, D. F. *Angew. Chem., Int. Ed.* **1999**, *38*, 429.
(2) Ziegler, K.; Holzkamp, E.; Breil, H.; Martin, H. *Angew. Chem.* **1955**, *67*, 541.
(3) For a recent review, see: Alt, H. G.; Köppl, A. *Chem. Rev.* **2000**, *100*, 1205.
(4) For a recent review, see: Nomura, K. *Recent Res. Dev. Pure Appl. Chem.* **1998**, *2*, 473.
(5) For a recent review, see: Ittel, S. D.; Johnson, L. K.; Brookhart, M. *Chem. Rev.* **2000**, *100*, 1169.
(6) van Beek, J. A. M.; van Doremaele, G. H. J.; Gruter, G. J. M.; Eggels, G. H. M. R. (DSM N. V.) WO-96/13529, 1996.
(7) Emrich, R.; Heinemann, O.; Jolly, P. W.; Krüger, C.; Verhovnik, G. P. J. *Organometallics* **1997**, *16*, 1511.
(8) Jolly, P. W.; Jonas, K.; Verhovnik, G. P. J.; Döhring, A.; Göhre, J.; Weber, J. C. (Studiengesellschaft Kohle m.b.H.) WO-A 98/04570, 1998.
(9) Döhring, A.; Göhre, J.; Jolly, P. W.; Kryger, B.; Rust, J.; Verhovnik, G. P. J. *Organometallics* **2000**, *19*, 388.
(10) Döhring, A.; Jensen, V. R.; Jolly, P. W.; Thiel, W.; Weber, J. C. In *Organometallic Catalysts and Olefin Polymerization*; Blom, R., Follestad, A., Rytter, E., Tilset, M., Ystenes, M., Eds.; Springer-Verlag: Oslo, Norway, 2000; p 127.
(11) Döhring, A.; Jensen, V. R.; Jolly, P. W.; Thiel, W.; Weber, J. C. *Organometallics* **2001**, *20*, 2234.

10.1021/om010525f CCC: $20.00
Publication on Web 10/11/2001

Scheme 1. Catalyst Precursors (1) and Assumed Active Species (2)

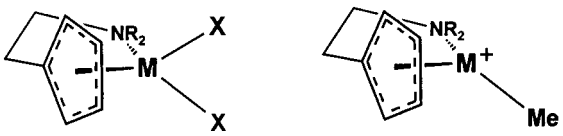

1 (X = Cl, Me) **2**

tion state III which could be potential olefin polymerization catalysts.

The aminoalkyl-substituted cyclopentadienyl−metal catalyst precursors are assumed to exist as dichloride or dimethyl compounds of type **1** (Scheme 1, R = alkyl group, M = transition metal Sc−Co) so that cobalt is the last of the first-row transition metals for which such a design is realistic. Activation of these catalyst precursors with methyl alumoxane (MAO) or with standard borane-based activators such as $B(C_6F_5)_3$ is assumed to generate the corresponding methyl cation, **2**, which serves as a first approximation to the active center in analogy with the group IV metallocene-based catalysts where the metal−alkyl cation has been identified as the active species.[12] A corresponding cation has not yet been observed for M(III)-based catalysts, but there are a number of indications[13] from the mechanistic investigations[14] of Cr(III) systems such as $[Cp^*(THF)_2CrMe]^+$-BPh_4^- that the active species have an analogous structure, viz., $[Cp(donor)CrR]^+$.

A computational study of the model system $[Cl(H_2O)CrMe]^+$ suggested that the olefin insertion for such cations should be facile, although less so than for corresponding cations with d^0 electron configuration.[15] The results for this simple model were further corroborated in calculations on a series of more realistic models of Cr(III)-based catalysts.[13] Further contributions to the understanding of early transition metal-based catalysts with formal d occupancy were published by the Ziegler group while the current work was in progress.[16,17] Their investigation of model catalytic systems with NH_2^- and NH_3 ligands[16] focused on the electronic effects of propagation and termination for high-spin d^1−d^4 first-row transition metals. A second contribution[17] treated catalysts with M(III) (M = Ti, V, and Cr) transition metal centers and diiminate ("NacNac") ligands, with particular emphasis on the product chain length. The calculated barriers to propagation and termination are rather similar for the NacNac systems, whereas a model diamide ligand yields significantly higher barriers to termination.

To investigate the electronic effects of the metal, we concentrate on a system containing a primary amino group, $[(\eta^1,\eta^5\text{-}H_2NC_2H_4C_5H_4)MMe]^+$, and attempt to identify trends among the lowest electronic states of the first-row transition metals (Sc−Co) in their ability to coordinate ethylene to take part in Cossee−Arlman[18−20] insertion. Therefore, only the first insertion step has been studied even though it is generally slower than subsequent insertion steps.[21] It is, however, reasonable to expect that the barriers to the first and subsequent insertion steps will show similar trends.[16] The current scan of the first-row transition metals is limited to ethylene as the monomer since a system that is not active toward ethylene insertion is not likely to display significant activity with higher or functionalized olefins. Furthermore, we are only concerned with the propagation reaction and do not treat the termination reaction; hence the product chain length is not considered. In addition to obtaining fundamental insight into the factors that govern the ease with which an olefin inserts into a metal−carbon bond, we hope that this work will inspire further experimental efforts to synthesize new M(III)-based catalysts.

2. Computational Details

We used gradient-corrected density functional theory (DFT) with the gradient corrections included self-consistently both during geometry optimization and energy evaluation. The local exchange−correlation potential developed by Vosko et al.[22] was employed and augmented with Becke's[23] nonlocal exchange corrections along with Perdew and Wang's[24] nonlocal correlation corrections. The resulting BPW91 functional was applied in the spin-unrestricted formulation (denoted UDFT) as implemented in the Gaussian 94 set of programs,[25] and stability tests of the resulting solutions were performed. Whereas the UDFT energies were used as is for high-spin states and low-spin states with little contamination, the energies of low-spin states with significant spin contamination were corrected according to the scheme described by Yamaguchi et al.,[26] to form what in the following will be termed CDFT energies. Contamination is assumed to arise from the next higher spin state (S+1) only,[27] and an explicit single-point calculation of this state must be performed to obtain the corresponding energy, E_{S+1}. The corrected energy, E_C, of the low-spin state (S) is obtained as

$$E_C \approx E_S + f_{SC}(E_S - E_{S+1}) \quad (1)$$

where E_S is the energy of the spin-contaminated solution and f_{SC} is the fraction of spin contamination approximated as

$$f_{SC} \approx \frac{\langle \hat{S}^2 \rangle_S - S(S+1)}{\langle \hat{S}^2 \rangle_{S+1} - \langle \hat{S}^2 \rangle_S} \quad (2)$$

$\langle S^2 \rangle_S$ and $\langle S^2 \rangle_{S+1}$ are the calculated spin expectation values for the low-spin state and the next higher spin state, respectively. In the derivation of eqs 1 and 2, the spin contamination of the

(12) Jordan, R. F.; Dasher, W. E.; Echols, S. F. *J. Am. Chem. Soc.* **1986**, *108*, 1718.
(13) Jensen, V. R.; Angermund, K.; Jolly, P. W.; Børve, K. J. *Organometallics* **2000**, *19*, 403.
(14) Theopold, K. H. *Chemtech* **1997**, *27*, 26.
(15) Jensen, V. R.; Børve, K. J. *Organometallics* **1997**, *16*, 2514.
(16) Schmid, R.; Ziegler, T. *Organometallics* **2000**, *19*, 2756.
(17) Deng, L. Q.; Schmid, R.; Ziegler, T. *Organometallics* **2000**, *19*, 3069.
(18) Cossee, P. *J. Catal.* **1964**, *3*, 80.
(19) Arlman, E. J. *J. Catal.* **1964**, *3*, 89.
(20) Arlman, E. J.; Cossee, P. *J. Catal.* **1964**, *3*, 99.
(21) Brookhart, M.; Volpe, A. F.; Lincoln, D. M. *J. Am. Chem. Soc.* **1990**, *112*, 5634.
(22) Vosko, S. H.; Wilk, L.; Nusair, M. *Can. J. Phys.* **1980**, *58*, 1200.
(23) Becke, A. D. *Phys. Rev. A* **1988**, *38*, 3098.
(24) Perdew, J. P.; Wang, Y. *Phys. Rev. B* **1992**, *45*, 13244.
(25) Frisch, M. J.; Trucks, G. W.; Schlegel, H. B.; Gill, P. M. W.; Johnson, B. G.; Robb, M. A.; Cheeseman, J. R.; Keith, T.; Petersson, G. A.; Montgomery, J. A.; Raghavachari, K.; Al-Laham, M. A.; Zakrzewski, V. G.; Ortiz, J. V.; Foresman, J. B.; Peng, C. Y.; Ayala, P. Y.; Chen, W.; Wong, M. W.; Andres, J. L.; Replogle, E. S.; Gomperts, R.; Martin, R. L.; Fox, D. J.; Binkley, J. S.; Defrees, D. J.; Baker, J.; Stewart, J. P.; Head-Gordon, M.; Gonzalez, C.; Pople, J. A. *Gaussian 94*; Gaussian, Inc.: Pittsburgh, PA, 1995.
(26) Yamaguchi, K.; Jensen, F.; Dorigo, A.; Houk, K. N. *Chem. Phys. Lett.* **1988**, *149*, 537.
(27) All the computed spin expectation values are close to those expected for the corresponding pure spin states (S) after annihilation of the first spin contaminant.

S+1 state is assumed to be negligible.[26] The above correction is currently applied whenever $f_{SC} > 0.05$. Tests of this correction scheme, and of the general performance of DFT methods concerning the relative stability of different spin surfaces of metal(III) complexes, are given in the Appendix. Compared with CASPT2 results, the energy profile of ethylene insertion for high-spin complexes seems to be accurately reproduced, whereas the stability of low-spin excited states is probably slightly overestimated at the CDFT level. The excellent agreement between gradient-corrected DFT and high-level ab initio methods in describing energy profiles for the Cossee−Arlman type[18−20] ethylene insertion step has also been noted previously for ground state d^0 titanium[28] and d^3 chromium[15] complexes.

Stationary points of ethylene insertion were optimized and characterized using algorithms involving analytic calculation of the first and second derivatives of the energy. Geometries were converged to a maximum force and displacement of 0.00045 hartree/bohr and 0.0018 bohr, respectively. Thermochemical values were computed within the harmonic-oscillator, rigid-rotor, and ideal-gas approximations. The basis sets employed were spherical-harmonics atom-centered Gaussian basis sets (denoted as basis B in ref 15) which contain a triply split d-shell on chromium and are of valence double-ζ plus polarization quality for first-row atoms and employ a doubly split 1s for hydrogen. Polarization functions were generally omitted for carbon atoms not forming part of the ethylene or the polymer chain. It has been specifically shown[15] that augmenting these sets with one contracted f-function on chromium and one uncontracted p-function on each hydrogen atom belonging to the growing alkyl chain or the monomer has very little effect on the calculated relative energies of ethylene insertion.

3. Results and Discussion

3.1. Geometric and Electronic Structure of the Catalyst Cation. A detailed description of the frontier orbitals has recently been given for the Cr d^3 catalyst cations[13] and for related complexes with d^1−d^4 occupancy.[16] Therefore we limit ourselves to a brief discussion based on the simple but instructive d^0 case to facilitate the subsequent discussion of the catalytic performance. An isosurface representation of the five lowest unoccupied molecular orbitals obtained for the $[(\eta^1,\eta^5\text{-}H_2NC_2H_4C_5H_4)ScMe]^+$ cation along with their energies is shown in Figure 1. The highest occupied orbital (HOMO, no. 44, not shown) has, as expected, metal−methyl bonding character.

The five orbitals 45−49 are seen to be dominated by metal d contributions. Double occupancy of the four lower-lying metal d orbitals (45−48) generates an 18-electron complex, and therefore a metal d-configuration (e.g., high-spin d^4) which leads to occupancy of all these orbitals is not expected either to interact appreciably with ethylene or to have a low barrier to insertion. The 18-electron rule is reflected in the large energy separation between orbitals 48 and 49, which is similar to that spanned by the four lower-lying d orbitals. The metal d orbitals in the other cationic $M(d^n)$ complexes are found to have shapes and relative energies qualitatively similar to those for $Sc(d^0)$. Subsequent discussions of electronic effects will therefore be based on the orbitals presented in Figure 1.

The electronic saturation, steric bulk, and rigidity imposed by the donor-substituted Cp-ligand causes the geometries of the ethylene-free complexes to be relatively uniform. Counting the amino group and the center of the Cp ring as two separate ligands, L and L′, the resulting $[MLL'R]^+$ cation has a somewhat higher affinity for a trigonal planar geometry than that found for corresponding transition metal cations with NH_2^- and NH_3 as ligands.[16] Half of the present species can be described as having a distorted trigonal planar structure (complexes with two, four, or five occupied metal d orbitals), while half of them adopt a weakly bent trigonal pyramidal shape (complexes with zero, one, or three occupied metal d orbitals).[29] A tendency toward a T-shape geometry, expected for high-spin d^4 complexes,[16,30] is seen for $Fe(^4A)$ (d^5 in four metal d orbitals) with a Cp−M−Me angle of 148°.

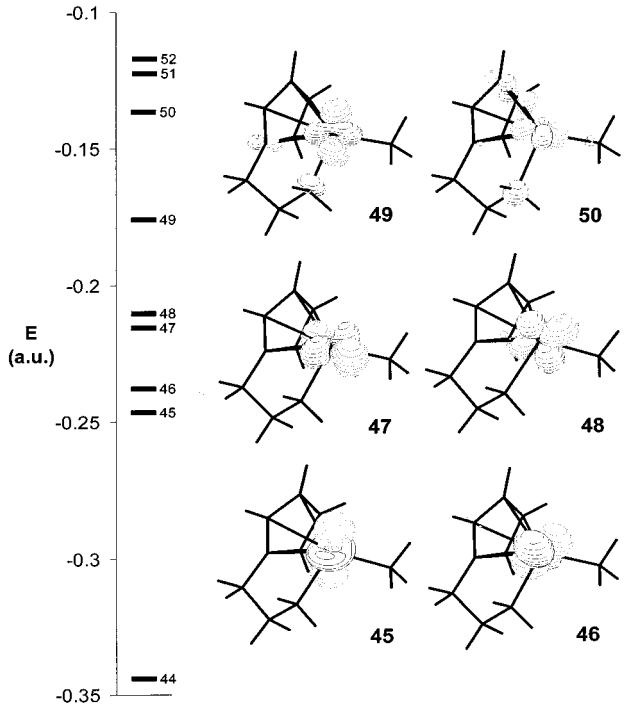

Figure 1. Energies and isosurfaces of the lowest unoccupied Kohn−Sham orbitals of $[(H_2NC_2H_4C_5H_4)ScMe]^+$. The orbitals are depicted as isosurfaces at a value of 0.09 au using the MOLDEN[67] program.

3.2. Ethylene Coordination and Insertion for the Individual Electronic States. In this section we will follow the coordination and insertion of ethylene as shown in Figure 2 for each of the low-lying electronic states of $[(H_2NC_2H_4C_5H_4)MMe]^+$ (M = Sc−Co) with the objective of identifying the electronic effects that contribute to a facile insertion reaction. Important DFT-optimized geometry parameters for the reactant (R), the π complex (π), and the transition state (TS) are given in Table 1, and the relative energies are listed in Table 2.

3.2.1. d^0 and d^1: Sc and Ti. A graphical representation of the relative energies of the reactants, π complex, and transition state of insertion for Sc and Ti is shown in Figure 3. In the case of $Sc(d^0)$, the metal−olefin bond

(28) Jensen, V. R.; Børve, K. J. *J. Comput. Chem.* **1998**, *19*, 947.

(29) An exception is $V(^1A)$, which is planar, probably as a result of spin contamination. The unrestricted solution for which the geometry was optimized is an almost equal mixture of singlet and triplet components.

(30) Albright, T. A.; Burdett, J. K.; Whangbo, M.-H. *Orbital Interactions in Chemistry*; John Wiley & Sons: New York, 1984.

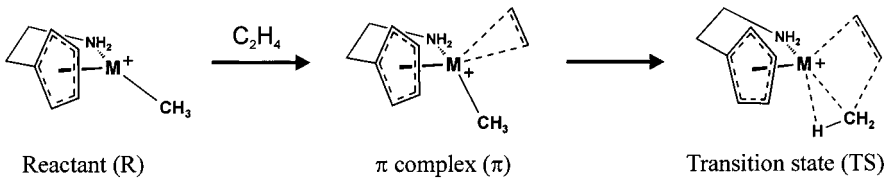

Figure 2. Reaction scheme for ethylene coordination and insertion as calculated for $[(H_2NC_2H_4C_5H_4)MMe]^+$ (M = Sc−Co). The three symbols R, π, and TS designate the reactant, the π complex, and the transition state of insertion, respectively.

Table 1. Important Structural Parameters of Stationary Points of Ethylene Insertion[a]

		M−C1		M−C2	M−C3			C1−C2			δR_{ag}[b]	Θ_p[c]
M	state	π	TS	π	R	π	TS	R	π	TS	TS	R
Sc	^{1}A	2.859	2.358	2.634	2.144	2.166	2.186	1.348	1.361	1.397	0.031	28.3
Ti	^{2}A	2.357	2.274	2.400	2.053	2.080	2.119	1.348	1.391	1.414	0.040	13.8
V	^{3}A	2.361	2.198	2.388	2.004	2.059	2.086	1.348	1.383	1.419	0.046	0.0
V	^{1}A	2.105	2.161	2.132	2.004	2.026	2.070	1.348	1.435	1.433	0.050	0.0
Cr	^{4}A	2.352	2.101	2.413	2.005	2.056	2.181	1.348	1.376	1.436	0.016	10.2
Cr	^{2}A	2.096	2.079	2.115	1.983	2.023	1.972	1.348	1.425	1.461	0.097	1.4
Mn	^{5}A	2.478	2.113	2.557	1.997	2.016	2.126	1.348	1.366	1.423	0.020	0.3
Mn	^{3}A	2.098	2.029	2.120	1.954	2.022	2.125	1.348	1.418	1.460	0.024	10.6
Mn	^{1}A	2.113	2.066	2.121	1.927	2.036	1.989	1.348	1.410	1.444	0.057	0.0
Fe	^{6}A	2.716	2.177	2.350	1.993	2.028	2.190	1.348	1.370	1.424	0.024	0.5
Fe	^{4}A	2.138	2.019	2.146	1.954	1.994	2.102	1.348	1.406	1.450	0.017	0.0
Fe	^{2}A	2.083	2.023	2.134	1.890	2.041	2.070	1.348	1.406	1.446	0.022	12.8
Co	^{3}A	2.179	2.016	2.215	1.932	1.983	2.069	1.348	1.387	1.442	0.020	0.0
Co	^{1}A	2.079	1.970	2.113	1.899	2.015	2.193	1.348	1.407	1.460	0.002	9.2

[a] Bond lengths in angstroms, angles in degrees. C1 and C2 denote the two ethylene carbons, with C1 being the atom forming a bond to the metal during insertion. C3 is the methyl carbon atom bonded to the metal in the reactant (R). π symbolizes the chromium−ethylene preinsertion complex and TS the transition state of insertion. [b] δR_{ag} = max{C−H} − min{C−H}, computed from C−H bond lengths pertaining to the agostic carbon atom. [c] $\Theta_p = 360° - \angle$CpMC3 − $\angle$CpMN − $\angle$NMC3, where Cp is represented by the geometric center of the five carbon atoms (average of the corresponding Cartesian coordinates).

Table 2. Calculated Relative Energies of Stationary Points of Ethylene Insertion[a]

		R			π			TS			
M	state	ΔE UDFT	$\langle S^2\rangle$	ΔE CDFT	ΔE UDFT	$\langle \hat{S}^2\rangle$	ΔE CDFT	ΔE UDFT	$\langle S^2\rangle$	ΔE CDFT	ΔE(TS−π)[b] UDFT[c]
Sc	^{1}A	0.0	0.00		−16.8	0.00		−12.6	0.00		4.1
Ti	^{2}A	0.0	0.76		−25.8	0.75		−12.7	0.76		13.1
V	^{3}A	0.0	2.03		−16.5	2.03		−9.6	2.03		6.9
V	^{1}A	9.0	0.97	16.2	−19.2	0.00		−0.8	0.92	8.9	28.1[c]
Cr	^{4}A	0.0	3.83		−19.8	3.82		−11.4	3.81		8.5
Cr	^{2}A	18.3	1.61	24.4	−10.8	0.79		4.1	0.77		14.9
Mn	^{5}A	0.0	6.08		−6.5	6.09		3.8	6.08		10.3
Mn	^{3}A	15.7	2.16		−17.0	2.07		4.6	2.05		21.6
Mn	^{1}A	25.5	0.66	27.5	−4.1	0.97	6.0	10.1	0.64	11.4	5.4[c]
Fe	^{6}A	20.4	8.76		10.9	8.77		25.1	8.77		14.2
Fe	^{4}A	0.0	3.80		−13.1	3.82		2.1	3.81		15.2
Fe	^{2}A	4.6	0.79		−19.8	0.77		−9.5	0.77		10.3
Co	^{3}A	0.0	2.02		−5.2	2.03		3.7	2.03		8.9
Co	^{1}A	0.3	0.00		−26.3	0.00		−11.9	0.00		14.4

[a] Electronic energies (kcal/mol) for the stationary points R, π, and TS are given relative to the lowest state for the separated reactants ethylene + $[(\eta^1,\eta^5\text{-}H_2NC_2H_4C_5H_4)MMe]^+$. $\langle S^2\rangle$ designates the expectation value of the S^2 operator, UDFT the unrestricted BPW91 energies, and CDFT the spin-corrected UDFT energies obtained as described in the Computational Details and the Appendix. [b] ΔE(TS−π) is the barrier to insertion from the π complex. [c] CDFT energies are used in cases where a correction for spin contamination has been performed, otherwise UDFT.

arises from charge−induced-dipole interactions and ethylene−metal σ donation,[31] without metal-to-olefin back-donation. Sc(d^0) has the lowest barrier to ethylene insertion calculated for the current systems and will serve as a reference for understanding the effect of formal d occupancy. The introduction of a single electron, d^1 (Ti), leads to some striking differences. In the naked metal cation, the unpaired electron occupies the lowest d orbital (no. 45 in Figure 1), which serves as acceptor orbital for the ethylene π electrons upon complexation. However, the cost of promoting the single d electron to the next higher level (46) upon ethylene coordination is small. Orbital 46, in turn, is responsible for π back-donation in the π complex, which results in a binding energy of ethylene some 9 kcal/mol larger than in the case of Sc. With a C1−C2 bond 4.3 pm longer than that of free ethylene, the accompanying weakening of the ethylene π bond is evident. The cost of breaking this back-donation bond enters into the barrier for ethylene insertion from the π complex, so that this barrier is 9 kcal/mol higher for titanium than for scandium.

3.2.2. d^2 and d^3: V and Cr. The high-spin d^2 V(^{3}A) system (Figure 4) has a considerably lower ethylene

(31) Jensen, V. R.; Børve, K. J.; Westberg, N.; Ystenes, M. *Organometallics* **1995**, *14*, 4349.

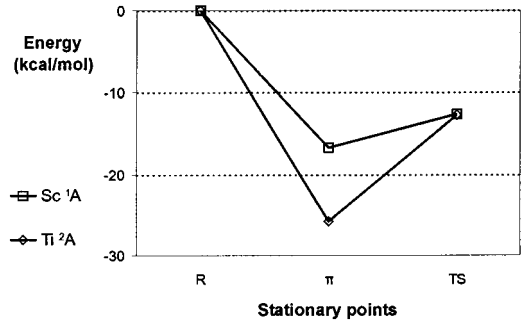

Figure 3. Energy profiles of ethylene insertion for M = Sc and Ti. The electronic energy is given relative to the infinitely separated ground state reactants, i.e., relative to ethylene + $(H_2NC_2H_4C_5H_4)MMe^+$.

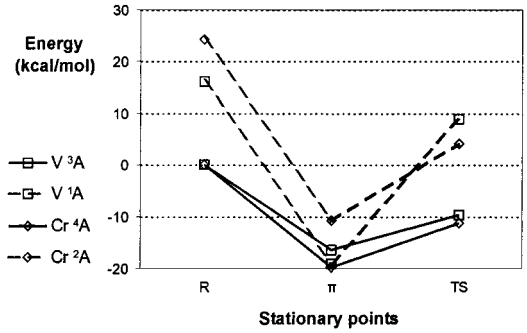

Figure 4. Energy profiles of ethylene insertion for M = V and Cr. The electronic energy is given relative to the infinitely separated ground state reactants, i.e., relative to ethylene + $[(H_2NC_2H_4C_5H_4)MMe]^+$.

binding energy than Ti mainly as a result of the cost of promoting one of the two unpaired electrons from the first to the third d-level (45 → 47) upon ethylene coordination. As expected, the weaker binding of ethylene contributes to a lower barrier to insertion for this state. Spin pairing in the vanadium d^2 system produces a potential curve for coordination and insertion similar to the d^1 Ti system, with even stronger binding of the monomer (and less favorable insertion) due to the formation of a regular Dewar−Chatt−Duncanson bond.[32,33] As a result of the latter bond, the low-spin π complex obtains a stability comparable to that of the high-spin counterpart, whereas the low-spin configuration is disfavored by as much as 16−19 kcal/mol for the reactant and the TS of insertion. The unfavorable spin pairing for the d^2 reactant is apparent from the similar energies of the two frontier orbitals 45 and 46 (Figure 1).

In comparison with V(^{3}A), the addition of another d electron in Cr(^{4}A) does not effect the coordination of ethylene to the high-spin cation much because the additional energy needed to make the acceptor orbital (45) available through promotion of an electron to orbital 48 instead of 47 is small (see Figure 1). The slightly higher ethylene binding energy found for Cr(^{4}A) is presumably associated with the larger charge−induced dipole interaction[31] resulting from the smaller size of chromium relative to vanadium. As in the case of V, spin pairing is unfavorable, especially for the reactants and the TS of insertion. The lack of electronic saturation in the low-spin Cr(^{2}A) complex leads to a strong metal−H agostic interaction in the TS of insertion which involves a low empty d orbital made available by spin pairing.

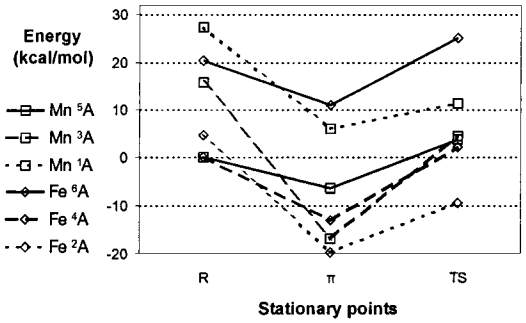

Figure 5. Energy profiles of ethylene insertion for M = Mn and Fe. The electronic energy is given relative to the infinitely separated ground state reactants, i.e., relative to ethylene + $[(H_2NC_2H_4C_5H_4)MMe]^+$.

3.2.3. d^4 and d^5: Mn and Fe. The introduction of another electron changes the situation significantly: in the high-spin configuration (Mn(^{5}A)), all four low-lying frontier orbitals now are occupied, and the 14 valence electrons of manganese are spread over the same number of molecular orbitals (9) as in an 18-electron complex. The calculations thus predict a considerable stability for the high-spin reactant (Figure 5) since a high-lying orbital (49) is necessarily involved in forming additional bonds. The high-spin, d^4 manganese−ethylene complex is bound by only 6.5 kcal/mol and is thus much weaker than the corresponding complexes of Ti(^{2}A), V(^{3}A), and Cr(^{4}A), where the ethylene binding energies are larger by 19.3, 10.0, and 13.3 kcal/mol, respectively. Stronger metal−ethylene bonds have been found for analogous high-spin cationic complexes of early transition metals (Ti−Mn) with small model ligands such as H_2O, NH_2^-, and NH_3[15,16] due to the reduced electronic saturation and steric hindrance imposed by the model ligands. These model complexes show a similar reduction in ethylene binding energy upon addition of d electrons as found here, however.[16] For Mn(^{5}A), the unstable nature of the π complex contributes to a reasonably low barrier to insertion (10.3 kcal/mol), although the low affinity for ethylene is expected to restrict the use of the Mn(^{5}A) cation as a catalyst (vide infra). The triplet surface of manganese, Mn(^{3}A), is rather high in energy at the reactant asymptote due to loss of exchange associated with the spin pairing in Mn(^{5}A) to vacate a relatively low lying frontier orbital (48). The latter orbital is occupied in the metal−ethylene complex which has a regular back-donation bond and is found to be energetically favorable with a substantial barrier to insertion. Further spin pairing to reach the singlet, Mn(^{1}A), surface is not preferred at any point during ethylene coordination and insertion.

Whereas the naked metal cation of the high-spin d^4 configuration has a significant stability, the addition of another electron with parallel spin is clearly unfavorable. In the high-spin d^5 configuration of Fe(^{6}A), the high-lying orbital 49 is occupied already in the 15-electron (10-orbital) reactant complex. The high-spin d^5 configuration is thus unfavorable both for the reactant

(32) Dewar, M. J. S. *Bull. Soc. Chim. Fr.* **1951**, *18*, C71.
(33) Chatt, J.; Duncanson, L. A. *J. Chem. Soc.* **1953**, 2939.

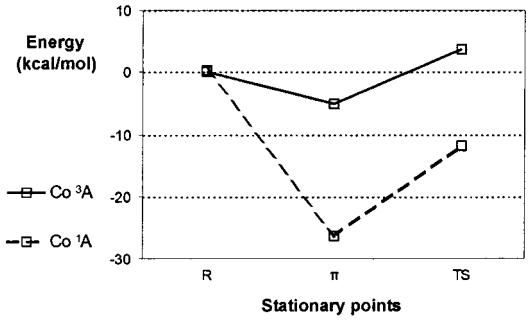

Figure 6. Energy profiles of ethylene insertion for M = Co. The electronic energy is given relative to the infinitely separated ground state reactants, i.e., relative to ethylene + $[(H_2NC_2H_4C_5H_4)MMe]^+$.

and for species having ethylene present in the coordination sphere of the metal. The lower-lying Fe(^{4}A) state involves a reactant with nine occupied orbitals, and this is the preferred configuration for the naked cation (as found for Mn(^{5}A)). Another parallel to the high-spin manganese complexes is that coordination and insertion of the olefin have to involve a high-lying frontier orbital (49). However, in the case of Fe(^{4}A), two electrons are available for π back-donation, and hence Fe(^{4}A) has a somewhat higher affinity for the olefin than Mn(^{5}A). Our calculations predict that further spin pairing will lead to more stable iron−ethylene structures, although the calculated doublet−quartet splitting for the π complex (6.7 kcal/mol) is within the expected accuracy of our calculations (see Appendix). The relatively low barrier to insertion for Fe(^{2}A) probably reflects the increasing stability of the 3d levels to the right of the transition series, associated with weaker back-donation.

3.2.4. d^6: Co. For the next metal, cobalt (Figure 6), reactant complexes having three or four occupied metal d frontier orbitals appear to have very similar energies. For coordination and insertion of the olefin, however, there is a clear preference for the closed shell singlet state. Due to this preference and the fact that the highest-spin state for iron (Fe(^{6}A)) was found to be rather unfavorable, Co(^{5}A) was not included in the present investigation. The Co(^{1}A) complexes can be compared to those of high-spin chromium: the three singly occupied orbitals in Cr are doubly occupied in Co and the metal valence electron count of the cobalt−ethylene complexes has reached 18. A somewhat higher ethylene binding energy and barrier to insertion is found for Co(^{1}A) compared to Cr(^{4}A) as a result of the back-donation by two electrons (rather than one).

3.2.5. Electronic Structure−Activity Relationships. In the previous sections we have focused on a small set of bonding interactions and electronic promotions prior to bond formation as the main factors behind the trends in the calculated ethylene binding energies and barriers to insertion. The arguments used for the general d^n case were to a large extent based on the simple d^0 and d^1 cases, where it is possible to resolve and identify the relevant contributions. We now present a simple expression for the metal−ethylene binding energy to test whether our simple promotion/donation/back-donation mechanism can be quantified for the general d^n case. Using increments derived from Sc(d^0) and Ti(d^1), we estimate the metal−ethylene binding energy ($\Delta E(\pi - R)$) as follows:

$$\Delta E(\pi - R) \approx \Delta E_\sigma(Sc) + n_\pi \Delta E_\pi(Ti) + \Delta E(LUMO - MO45)_\alpha + \Delta E(LUMO - MO45)_\beta \quad (3)$$

ΔE_σ(Sc) designates the contribution originating from σ donation and is assumed to be constant and identical to the binding energy in the simple d^0 case ($\Delta E_\sigma \approx \Delta E_\sigma(Sc) = \Delta E(\pi - R)(Sc) = -16.8$ kcal/mol). ΔE_σ(Sc) includes of course also other contributions such as the charge−induced-dipole interaction[31] and the deformation of the naked metal cation upon formation of the metal−ethylene complex. ΔE_π(Ti) is the contribution from back-donation by one electron as estimated from the Ti case ($\Delta E_\pi(Ti) \approx \Delta E(\pi - R)(Ti) - \Delta E_\sigma(Sc) - \Delta E(MO46 - MO45)_\alpha = -14.6$ kcal/mol), whereas n_π is the number of electrons involved in back-donation. $\Delta E(LUMO - MO45)_\alpha$ is the energy difference between the lowest unoccupied α orbital and the best acceptor α orbital (no. 45, see Figure 1) and is best thought of as an electronic preparation prior to bond formation in the form of promotion of an electron from the MO45 to the LUMO. $\Delta E(LUMO - MO45)_\beta$ is the corresponding promotion energy for any β-spin electron in MO45. Through application of eq 3 in combination with the orbital energies calculated for the scandium cation (see Figure 1) it is possible to reproduce the major trends for the ethylene coordination energy for the first transition row (see Figure 7), which thus confirms that the described mechanism is adequate for a qualitative understanding of these variations. A quantitative agreement with the DFT results cannot be expected, of course, since ΔE_σ, ΔE_π, and the orbital energy levels used to calculate the promotion energies are kept constant for all metals considered. A particularly large discrepancy is found for Fe(^{6}A), the only state for which a 10-orbital complex is realized already at the reactant asymptote.

Turning now to the barrier to insertion as calculated from the π complex, we already pointed out (section 3.2.1) that the back-donation bond must be broken for ethylene to insert and that the barrier from the π complex should therefore correlate with the ethylene binding energy (see Figure 8). When going from the π complex to the transition state, the back-donation orbital evolves into an orbital with predominant metal d character and is thus destabilized (as first pointed out in ref 13), and a larger destabilization of this orbital will then imply a higher insertion barrier.[16] The influence of back-donation is also reflected geometrically in the C1−C2 bond lengths: for example, they increase upon complexation by 1.3, 4.3, and 8.7 pm for Sc(^{1}A), Ti(^{2}A), and V(^{1}A), respectively, with a concomitant increase of the barriers (4.1, 13.1, and 28.1 kcal/mol; back-donation involving 0, 1, and 2 electrons). Furthermore, the high-spin d^2 and d^3 complexes of V and Cr show relatively small increases in the C1−C2 bond length (2.8−3.5 pm) upon coordination and have low barriers (<10 kcal/mol) to insertion. It should be noted that electron pairing does not necessarily result in insertion barriers as large as those calculated for the low-spin vanadium complex. This is particularly true for the late metals (Fe and Co) for which back-donation is less favorable due to d-level stabilization.

3.2.6. Allowing for Spin Crossing. So far we have assumed that spin multiplicity is conserved during the

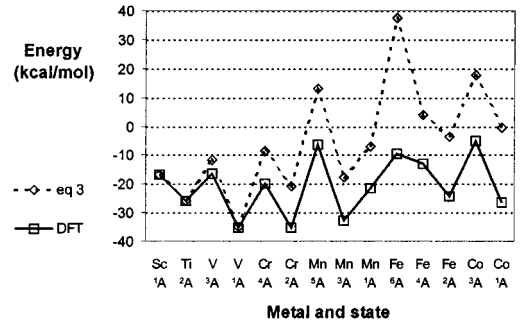

Figure 7. Ethylene coordination energy ($\Delta E(\pi - R)$) for the individual electronic states of the metals Sc−Co as obtained from DFT and estimated using eq 3.

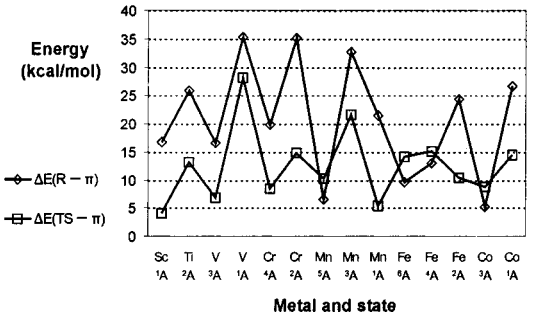

Figure 8. Ethylene bond energy ($\Delta E(R - \pi)$) and barrier to insertion from the π complex ($\Delta E(TS - \pi)$) for the individual electronic states of the metals Sc−Co as obtained from DFT.

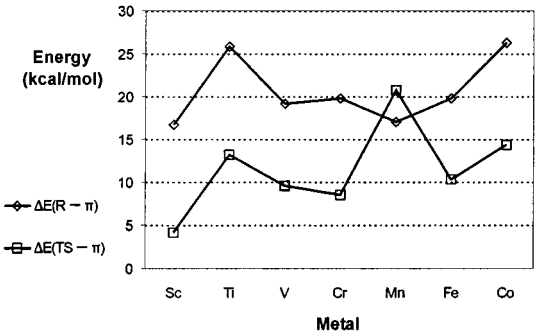

Figure 9. Metal−ethylene bond energy ($\Delta E(R - \pi)$) and barrier to insertion from the π complex ($\Delta E(TS - \pi)$) for the metals Sc−Co using the lowest spin state for each stationary point (allowing for spin crossing).

reactions considered. However, there is a rapidly growing number of examples of organometallic reactions that involve more than one spin surface.[34] The first-row transition metal systems may be particularly prone to undergo spin inversion due to the intermediate degree of spin−orbit coupling expected for these elements.[34] In the following discussion we will not explicitly investigate spin inversion for the title systems but rather consider the possible effects arising from crossing between the calculated potential energy surfaces corresponding to different spin states for each metal assuming that spin inversion itself is not a restriction. The resulting electronic ethylene binding energies ($\Delta E(R - \pi)$) and barriers to insertion ($\Delta E(TS - \pi)$) are shown in Figure 9. Based upon the current DFT energies, spin crossing could influence the energy profile of ethylene coordination and insertion for the metals V, Mn, Fe, and Co. A large effect will, however, be expected only in the case of Mn. The high-spin d^4 configuration of the Mn reactant is particularly stable, and as a result, a relatively low ethylene binding energy is observed even for the triplet Dewar−Chatt−Duncanson-type manganese−ethylene complex. A particularly large barrier thus results during insertion because it is necessary to cleave a strong back-donation bond. A second spin crossing to return to the quintet surface does not ameliorate the situation because the ^{5}A state is of equally high energy. The four d electrons occupy all low-lying frontier orbitals 45−48, thus hampering the bond formation in the TS region. For the other metals, the obvious correlation between metal−ethylene bond strength and barrier height has already been commented upon above (sections 3.2.1 and 3.2.5).

(34) Schröder, D.; Shaik, S.; Schwarz, H. *Acc. Chem. Res.* **2000**, *33*, 139.

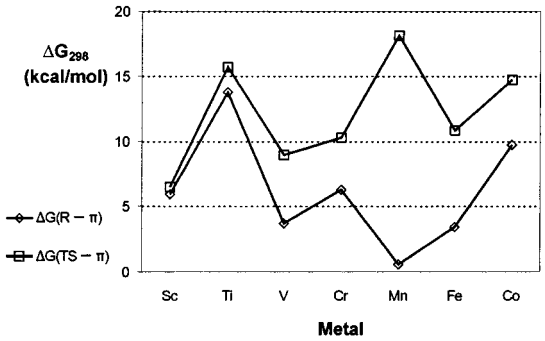

Figure 10. Gibbs free energy at 25 °C for the reactant $\Delta G(R - \pi)$ and TS of insertion $\Delta G(TS - \pi)$ given relative to the ground state π complex for the metals Sc−Co.

3.3. Comparison with Experimental Results. The only experimentally observed energy values available for direct comparison with our calculations stem from investigations of the cobalt−alkyl cations Cp*(donor)-Co−R^+ (Cp* = C_5Me_5) reported by Brookhart et al.[21,35−38] ^{13}C NMR-based kinetic analysis of the ($^{13}C_2H_4$-enriched) ethylene polymerization reaction for [Cp*(P(OMe)$_3$)-$CoC_2H_5]^+BF_4^-$ in CD_2Cl_2[21] gave a free energy of activation for insertion from the π complex of 14.3 ± 0.2 kcal/mol. This value is in excellent agreement with our results ($\Delta G^{\ddagger}$ = 14.7 kcal/mol, Figure 10) for the $[(H_2NC_2H_4C_5H_4)CoMe]^+$ cation. The near perfect agreement between theory and experiment is partly fortuitous since the two values have not been obtained for identical chemical systems, but it would still seem to indicate that our computational approach (which neglects effects associated with the counterion and solvent) is adequate for the current purposes.

For the remaining metals, only qualitative comparisons with observed activities can be made. In the case of Ti, the donor-substituted Cp complexes, analogues to those reported for chromium,[9,10] have been studied as olefin polymerization catalysts,[6] and although activation energies have not been given, satisfactory activities are observed only at elevated temperatures. For example,

(35) Schmidt, G. F.; Brookhart, M. *J. Am. Chem. Soc.* **1985**, *107*, 1443.
(36) Brookhart, M.; Lincoln, D. M.; Volpe, A. F.; Schmidt, G. F. *Organometallics* **1989**, *8*, 1212.
(37) Brookhart, M.; Desimone, J. M.; Grant, B. E.; Tanner, M. J. *Macromolecules* **1995**, *28*, 5378.
(38) Tanner, M. J.; Brookhart, M.; DeSimone, J. M. *J. Am. Chem. Soc.* **1997**, *119*, 7617.

for the *N*-pyrrolidinylethyl-substituted complex, (*cyclo*-$C_4H_8NC_2H_4C_5Me_4$)$TiCl_2$, activities of about 216 and 575 kg PE/mol Ti·h·bar are reported at 80 and 115 °C, respectively (P = 8 bar; Al:Ti = 2000:1), while at 21 °C this compound has an activity of only 6 kg PE/mol Ti·h·bar (P = 2.05 bar; Al:Ti = 104:1).[39] This suggests that the activity of the Ti analogues of the donor-substituted Cp complexes is highly dependent on the polymerization temperature, i.e., that the activation energy must be high as predicted by our calculated barriers. It should be mentioned that at high temperatures a strong binding of ethylene prior to insertion may be an advantage. With the π complex as the undisputed resting state even at high temperatures, the unfavorable $-T\Delta S$ term of the coordination will not add to the free energy of activation. At 25 °C the Gibbs free energy of ethylene coordination is −13.8 kcal/mol (Figure 10), and this increases to −9.7 kcal/mol at 140 °C, implying that the zero-point and temperature corrections to give free energies amount to 12 kcal/mol at 25 °C and that the increase in temperature leads to a destabilization of the metal−ethylene complex (and the TS) of 4.1 kcal/mol. The remaining catalysts all have less negative free energies of ethylene coordination (assuming spin crossing is not a restriction). The presence of larger substituents (e.g., methyl groups) on the nitrogen atom and a longer growing chain will contribute to favoring the reactant asymptote (vide infra). For more realistic catalytic complexes such as $[(Me_2NC_2H_4C_5H_4)MR]^+$, it could well be that Ti is the only metal for which the π complex acts as resting state at elevated temperatures. For the other metals, the loss of entropy during coordination will thus have a direct effect on $\Delta G^{\ddagger}$.

The barriers to insertion from the π complex calculated for Cr(III)−alkyl cations found here as well as in previous studies[13,15] all lie close to the activation energy measured (8 kcal/mol) by Theopold et al.[40] for ethylene polymerization using $[Cp^*(THF)_2CrMe]^+BPh_4^-$. However, the similarity in free energy between the separated reactants and the π complex for realistic M(III)-based catalytic systems as noted above makes it difficult to claim that the insertion from the π complex constitutes the rate-determining step. In the present comparison of different metals it suffices to mention that chromium clearly belongs to the metals for which a relatively facile coordination and insertion of ethylene is predicted. This is consistent with the activity toward ethylene polymerization typically observed for Cr(III) compounds in general[41] and the very high activity toward ethylene polymerization observed for the amino-substituted Cp catalysts[9] as well as the equally high activity toward ethylene oligomerization observed for the phosphino-substituted Cp systems[10] in particular. Furthermore, the recent progress in the construction of well-defined, homogeneous V(III)-based catalysts for the oligomerization[42] and polymerization[43−45] of ethylene is not surprising in light of the current computational results for this metal reported here.

The particularly facile coordination and insertion of ethylene predicted for Sc should be worth pursuing. However, apart from the neutral, monoalkyl L_2ScR (L = (substituted) cyclopentadienyl ligand) compounds[46−50] that have predominantly been employed as models for the metallocene cations of group IV, $[L_2MR]^+$, few catalytically active complexes of scandium with more than one alkyl or halide ligand have been reported, and in none of these cases have explicit activity data been given. Dialkyl Sc(III) complexes with an amido diphosphine ligand, $[N(SiMe_2CH_2P^iPr_2)_2]ScR_2$, have been reported to catalyze the formation of polyethylene without the need for activation.[51] The application of other monoanionic ligands, of the β-diketiminato, "NacNac"-type, has also given dialkyl complexes of Sc(III)[52,53] which polymerize ethylene without the need for activation, although treatment with a standard activator such as $B(C_6F_5)_3$ enhances the activity. In addition, a trialkyl complex of Sc(III), based on the neutral 1,4,7-trimethyl-1,4,7-triazacyclononane ligand, has been reported.[54] Like the NacNac systems, the triazacyclononane complex can be activated to give complexes that exhibit olefin polymerization chemistry. Motivated by the high activity predicted by the calculations, scandium derivatives of the aminoalkyl-substituted Cp ligands (successfully applied for Ti and Cr) have been tested as ethylene polymerization catalysts:[55] preliminary results indicate that, in the presence of MAO, the Sc(III) dialkyls catalyze the formation of short-chain (C_4−C_{10}) oligomers with medium[1] (10−100 g product $mmol^{-1}$ bar^{-1}) activity.

3.4. Potential New Catalysts. Having established that our computational results are consistent with the observed activity of existing M(III)-based catalysts, we believe that our predictions for metals for which oxidation state III has been neglected with respect to olefin polymerization can be used as a qualitative guide to their potential activity.

Whereas titanium(III) and chromium(III) in the form of the recently developed homogeneous, MAO-activated

(39) Döhring, A.; Jolly, P. W. Unpublished results. Under the same mild conditions, the Cr-analogue displays an activity of 3585 kg PE/mol Cr·h·bar.[9]

(40) Thomas, B. J.; Noh, S. K.; Schulte, G. K.; Sendlinger, S. C.; Theopold, K. H. *J. Am. Chem. Soc.* **1991**, *113*, 893.

(41) Theopold, K. H. *Eur. J. Inorg. Chem.* **1998**, 15.

(42) Brussee, E. A. C.; Meetsma, A.; Hessen, B.; Teuben, J. H. *Chem. Commun.* **2000**, 497.

(43) Brandsma, M. J. R.; Brussee, E. A. C.; Meetsma, A.; Hessen, B.; Teuben, J. H. *Eur. J. Inorg. Chem.* **1998**, 1867.

(44) Kim, W. K.; Fevola, M. J.; Liable-Sands, L. M.; Rheingold, A. L.; Theopold, K. H. *Organometallics* **1998**, *17*, 4541.

(45) Yasuda, H.; Ihara, E.; Fujimura, T.; Maeno, Y.; Ogata, K.; Sato, Y.; Desurmond, G. *J. Synth. Org. Chem. Jpn.* **2000**, *58*, 1084.

(46) Piers, W. E.; Shapiro, P. J.; Bunel, E. E.; Bercaw, J. E. *Synlett* **1990**, 74.

(47) Shapiro, P. J.; Bunel, E.; Schaefer, W. P.; Bercaw, J. E. *Organometallics* **1990**, *9*, 867.

(48) Burger, B. J.; Thompson, M. E.; Cotter, W. D.; Bercaw, J. E. *J. Am. Chem. Soc.* **1990**, *112*, 1566.

(49) Hajela, S.; Bercaw, J. E. *Organometallics* **1994**, *13*, 1147.

(50) Shapiro, P. J.; Cotter, W. D.; Schaefer, W. P.; Labinger, J. A.; Bercaw, J. E. *J. Am. Chem. Soc.* **1994**, *116*, 4623.

(51) Fryzuk, M. D.; Giesbrecht, G.; Rettig, S. J. *Organometallics* **1996**, *15*, 3329.

(52) Lee, L. W. M.; Piers, W. E.; Elsegood, M. R. J.; Clegg, W.; Parvez, M. *Organometallics* **1999**, *18*, 2947.

(53) Knight, L. K.; Hayes, P. G.; Lee, L. W. M.; Piers, W. E.; Parvez, M.; Clegg, W.; Elsegood, M. R. J. In *Book of Abstracts, Organometallic Catalysts and Olefin Polymerization*: Oslo, Norway, 2000.

(54) Hajela, S.; Schaefer, W. P.; Bercaw, J. E. *J. Organomet. Chem.* **1997**, *532*, 45.

(55) Döhring, A.; Holle, S.; Jensen, V. R.; Jolly, P. W. Unpublished results. The amino-substituted cyclopentadienylscandium dichlorides were obtained by reaction of $Sc(THF)_3Cl_3$ with the appropriate alkalimetal cyclopentadienyl derivatives as described for Cr.[9] For the *N*-pyrrolidinylethyl-substituted complex, (*cyclo*-$C_4H_8NC_2H_4C_5Me_4$)-$ScCl_2$, the dimethyl analogue was obtained after treatment with $MgClCH_3$. At 21 °C and 2 bar the dimethyl complex was found to oligomerize (96% 1-butene) ethylene with an activity of 42 kg product/mol Sc·h in toluene.

catalysts based on donor-substituted Cp ligands have proved their potential in olefin polymerization, high activities have not yet been realized for metals such as scandium, vanadium, and cobalt. Nevertheless, our calculations suggest that such a potential does exist for these metals. Foremost among our predictions is, without doubt, scandium. Sc and the other metals of group III have as yet received relatively little attention as homogeneous catalysts, and given the promising activity obtained by simply applying a ligand designed for a different metal (Cr),[55] it is likely that significant improvements in activity could be obtained through optimization of the ligands. It is conceivable that the product chain length can also be increased since, in the case of Cr with phosphinoalkyl-substituted cyclopentadienyl ligands, it has been shown that the product can vary from 1-butene to mainly polyethylene simply by increasing the size of the two alkyl substituents on the phosphorus atom.[10,11]

Our results also suggest that vanadium(III) should have a catalytic potential similar to that of chromium(III), and reports of well-defined V(III)-based catalysts have recently started to appear. In the case of Co(III), for which well-defined catalysts are limited to the alkyl cations $[Cp^*(donor)CrR]^+$ ($Cp^* = C_5Me_5$), application has so far been directed toward mechanistic studies. We have already pointed out the electronic similarities between Cr and Co for the metal−methyl reactant cations. For chromium, the particularly high activity of the MAO-activated catalysts containing amino- or phosphinoalkyl-substituted cyclopentadienyl ligands has been attributed[13] to the fact that the donor is bridged to the anionic ligand, suggesting that a similar ligand design might be attractive also for cobalt. Furthermore, the calculated energy differences are similar to those of Ti and show a relatively large barrier to ethylene insertion from the π complex. If complexes of sufficient thermal stability can be designed, cobalt(III) could have some potential as a catalyst at elevated temperatures.

Among the first-row transition metals, only in the case of Mn and Fe have well-defined catalysts of oxidation state III yet to be reported. In the case of manganese the combination of low stability for the π complex and a high barrier to insertion, both resulting from the high degree of electronic saturation in the reactant cation, suggests that this metal will not form active catalysts. In the case of iron, a relatively low stability of the π complex as well as an electronic barrier to insertion higher than 10 kcal/mol can be noted. Our calculations do not exclude significant activity for this metal, but the results suggest a larger potential for Sc and V.

Appendix

Our previous benchmark tests of methods applied to metal-catalyzed ethylene insertion have been concerned with ground states only.[15,28] The present comparison of different spin states calls for additional tests with a particular focus on the DFT description of the relative stability of different spin states for relevant metal complexes. That such benchmark tests should be of general interest is underscored by the recent contribution from Khoroshun et al.[56] on Fe(II)-based catalysts for olefin polymerization and oligomerization. They point to the fact that pure DFT and hybrid functionals such as B3LYP tend to predict very different energy separations between spin states, the introduction of Hartree−Fock exchange generally favoring the high-spin states. They conclude that rigorous benchmark calibration tests are needed and that an appropriate test system should have a realistic coordination number so as to avoid the established problem with the DFT description of the relative stability of s^0d^n and s^1d^{n-1} configurations. We chose the quartet and doublet potential energy surfaces of chromium for further investigation. To make treatments with high-level wave function-correlated methods tractable, a small model catalyst, $[H(NH_3)CrMe]^+$, was used instead of the more realistic $[(\eta^1,\eta^5\text{-}H_2NC_2H_4C_5H_4)CrMe]^+$. The applicability of the small model system is demonstrated by the fact that the adiabatic $^2A \leftarrow {}^4A$ transition energy is calculated (UDFT) to be 22.4 kcal/mol for the small, ethylene-free model system, only 4.1 kcal/mol higher than that found for the larger system (Table 2). Furthermore, the Mulliken d population of Cr is calculated to be 4.6 e in both the doublet and quartet states of the large as well as the small system. Thus, the coordination environment chosen for the small model system seems to be realistic for the investigation of electronic effects.

Multireference second-order perturbation theory with a g1-corrected zeroth-order Hamiltonian (CASPT2[g1][57]) was employed in a single-point fashion (using the UDFT geometries) in order to obtain accurate estimates of the nonisogyric relative energies between the two potential curves, ^2A and ^4A. The g1, g2, and g3 zeroth-order Hamiltonians have been designed to give a balanced treatment of reference functions dominated by closed- and open-shell configurations, respectively, and typically reduce the errors of calculated excitation energies to well below 1 kcal/mol compared to corresponding full CI and MRCI values.[57] The calculations were performed using the MOLCAS 4.1[58] set of programs, and the basis sets consisted of spherical-harmonics, atom-centered Gaussian functions of the atomic natural orbitals (ANO) type as provided in the MOLCAS basis set library. For chromium, a (21s15p10d6f) primitive basis contracted to [6s5p4d3f] was used.[59] Nitrogen and carbon atoms were described by (14s9p4d)/[4s3p2d] basis sets.[60] The hydrogen atom covalently bonded to Cr was described by a (8s4p3d)/[3s2p] basis set,[60] whereas for the other H atoms, a [3s1p] contraction was employed.

Considering first the naked cation, $[H(NH_3)CrMe]^+$, the active orbital space in the CASSCF wave function included the σ and σ^* orbitals pertaining to the chromium−methyl and chromium−hydrogen bonds along with three metal d orbitals. With the three d electrons of Cr and the two covalent chromium−ligand bonds

(56) Khoroshun, D. V.; Musaev, D. G.; Vreven, T.; Morokuma, K. *Organometallics* **2001**, *20*, 2007.
(57) Andersson, K. *Theor. Chim. Acta* **1995**, *91*, 31.
(58) Andersson, K.; Blomberg, M. R. A.; Fülscher, M. P.; Karlström, G.; Kellö, V.; Lindh, R.; Malmqvist, P.-Å.; Noga, J.; Olsen, J.; Roos, B. O.; Sadlej, A. J.; Schütz, M.; Seijo, L.; Siegbahn, P. E. M.; Urban, M.; Widmark, P.-O. *MOLCAS*, version 4.1; Department of Theoretical Chemistry, Chemistry Center, University of Lund: Lund, Sweden, 1996.
(59) Pou-Amérigo, R.; Merchán, M.; Nebot-Gil, I.; Widmark, P.-O.; Roos, B. O. *Theor. Chim. Acta* **1995**, *92*, 149.
(60) Widmark, P.-O.; Malmqvist, P.-Å.; Roos, B. O. *Theor. Chim. Acta* **1990**, *77*, 291.

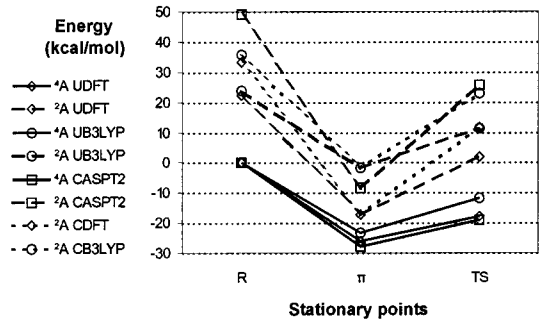

Figure 11. Energy profiles of ethylene insertion into the Cr−C bond of $[H(NH_3)CrMe]^+$ at various levels of theory. The electronic energy is given relative to infinitely separated ground state reactants, i.e., relative to ethylene + $[H(NH_3)CrMe]^+$.

Table 3. Calculated Relative Energies of Ethylene Coordination and Insertion into the Cr−C Bond of $[H(NH_3)CrMe]^+$[a]

method	state	R	π	TS
UDFT[b]	^{4}A	0.0 (3.84)	−25.9 (3.84)	−17.9 (3.83)
UDFT[b]	^{2}A	22.4 (1.75)	−17.2 (0.80)	1.9 (1.76)
CDFT	^{2}A	33.4	−17.2	11.7
UB3LYP[b]	^{4}A	0.0 (3.89)	−23.2 (3.88)	−11.8 (3.87)
UB3LYP[b]	^{2}A	23.9 (1.75)	−1.7 (0.87)	11.5 (1.76)
CB3LYP	^{2}A	35.7	−1.7	22.8
CASSCF	^{4}A	0.0	−11.4	8.9
CASSCF	^{2}A	44.3	21.9	52.3
CASPT2[c]	^{4}A	0.0	−27.9	−19.2
CASPT2[c]	^{2}A	49.2	−8.4	25.8

[a] Electronic energies (kcal/mol) are given relative to infinitely separated ground state reactants (R), i.e., relative to ethylene + $[H(NH_3)CrMe]^+$. [b] The calculated expectation value of the S^2 operator is given in parentheses. [c] On a Compaq ES40 with 667 MHz Alpha processors, a single-point calculation for π or TS typically requires 6−8 h for CASPT2, compared with less than 10 min for UDFT.

contributing two electrons each, this leads to a CASSCF model space denoted as CASSCF(7,7). For free ethylene, the two π electrons were correlated and the active orbital space consisted of the π and π^* orbitals, leading to a CASSCF(2,2) description. For the metal−ethylene complex as well as for the TS of insertion, orbitals corresponding to the active orbitals of the naked catalyst cation and free ethylene were identified and included in the active space, leading to a CASSCF(9,9) description. All valence electrons were correlated in the subsequent CASPT2[g1] calculations. The CASSCF wave function was in all cases found to be a good zeroth-order representation, with weights in the range 0.77−0.85 for the metal complexes and 0.91 for ethylene. The second-order perturbation corrections are thus likely to be valid and should lead to the accuracy normally expected for CASPT2[g1].[57] These CASPT2 calculations were furthermore reasonable in terms of CPU time.

In Table 3 and Figure 11 the CASPT2[g1] results are compared to the UDFT/B energies (basis B, see Computational Details) as well as to single-point UB3LYP/B energies. UB3LYP denotes the unrestricted version of the three-parameter hybrid density functional method due to Becke,[61] as implemented in the Gaussian 94 set of programs.[25] For the quartet ground state stationary points, the same picture emerges as found previously when comparing different methods for ethylene insertion for d^3 and d^0 transition metal complexes:[15,28] DFT methods, in particular pure, gradient-corrected DFT functionals such as BPW91, give relative energies in excellent agreement with the best ab initio methods available. The hybrid B3LYP method also performs well, but apparently includes less dynamic correlation than the pure, gradient-corrected functionals and thus gives energies relative to separated reactants a few (7 in the present case) kcal/mol higher for the relatively tight transition state structures than do the reference ab initio methods.

The relative stabilities of the two spin states obtained with the two density functional-based methods are less convincing when compared to the CASPT2[g1] results. As expected UB3LYP is found to predict a somewhat larger quartet−doublet separation than the pure UDFT method, and for the π complex, the quartet−doublet separation is also larger than that of CASPT2[g1]. The performance of UB3LYP and UDFT is particularly poor for the reactants and the transition state of insertion for which both methods significantly underestimate the quartet−doublet separation. These large deviations coincide with high expectation values for S^2 obtained in the density functional-based calculations, suggesting that some of the difference is caused by spin contamination of the doublet solutions. Approximate removal of the contamination of the UDFT doublet solutions to form the energies here labeled as CDFT was thus performed for the reactants and the transition state of insertion following the scheme of Yamaguchi et al.[26] as outlined in the Computational Details. The correction for spin contamination is seen to improve significantly the UDFT energies for the doublet, leading to a profile more parallel to the CASPT2[g1] curve although still uniformly lower in energy. Similarly, the UB3LYP energies also benefit from such a correction. The resulting CB3LYP energies agree well with the CASPT2[g1] results, although with less systematic deviations than for UDFT.

Augmentation of the basis sets used in the CASPT2-[g1] calculations is likely to lower this doublet curve somewhat, but presumably not sufficiently to coincide with the CDFT profile. Our validation calculations thus indicate that an approach based on unrestricted BPW91 (termed UDFT) energies for the high-spin states and corrected (CDFT) energies for the contaminated low-spin states should give accurate results for high-spin ground state surfaces and a limited and systematic overestimation of the stability for low-spin excited states.

The applicability of the chosen correction scheme[26] to quartet−doublet gaps corroborates the positive experiences already made for singlet−triplet gaps.[26,62,63] On the other hand, it is known that this correction for spin contamination is less successful for homolytic bond dissociation processes,[64−66] which, however, should not be relevant for our present study.

(61) Becke, A. D. *J. Chem. Phys.* **1993**, *98*, 5648.
(62) Yamanaka, S.; Kawakami, T.; Nagao, H.; Yamaguchi, K. *Chem. Phys. Lett.* **1994**, *231*, 25.
(63) Garavelli, M.; Bernardi, F.; Olivucci, M.; Robb, M. A. *J. Am. Chem. Soc.* **1998**, *120*, 10210.
(64) Wittbrodt, J. M.; Schlegel, H. B. *J. Chem. Phys.* **1996**, *105*, 6574.
(65) Goldstein, E.; Beno, B.; Houk, K. N. *J. Am. Chem. Soc.* **1996**, *118*, 6036.
(66) Davidson, E. R. *Chem. Phys. Lett.* **1998**, *284*, 301.
(67) Schaftenaar, G. *MOLDEN*, version 3.5; University of Nijmegen: Nijmegen, The Netherlands, 1999.

Acknowledgment. This research was financially supported by the Research Council of Norway (grant no. 119204/410). Access to supercomputer resources was granted by the Research Council of Norway (Programme for Supercomputing), the Rechenzentrum der Gesellschaft für Wissenschaftliche Datenverarbeitung in Göttingen, the Max-Planck-Institute for Biological Cybernetics in Tübingen, and the Rechenzentrum der MPG und IPP in Garching. We thank Prof. P. W. Jolly for helpful suggestions and discussions.

OM010525F